Supporting Information

Active cargo loading into extracellular vesicles: highlights the heterogeneous encapsulation behavior

Chaoxiang Chen [a,], Mengdi Sun [a], Jialin Wang [a], Liyun Su [b], Junjie Lin [a] and Xiaomei Yan [b,]**

[a] Department of Biological Engineering, College of Food and Biological Engineering, Jimei University, Xiamen, Fujian 361021, People's Republic of China

[b] Department of Chemical Biology, MOE Key Laboratory of Spectrochemical Analysis & Instrumentation, Key Laboratory for Chemical Biology of Fujian Province, Collaborative Innovation Center of Chemistry for Energy Materials, College of Chemistry and Chemical Engineering, Xiamen University, Xiamen, Fujian 361005, People's Republic of China

* To whom correspondence should be addressed. E-mail: cxchen@jmu.edu.cn, xmyan@xmu.edu.cn,

1. Investigation of the encapsulation efficiency of Dox-LPs prepared by SEAL.

Doxorubicin loaded liposomes (Dox-LPs) were prepared by film hydration and extrusion method. Briefly, 1,2-dioleoyl-sn-glycero-3-phosphocholine (DOPC) and cholesterol (3:2 mol/mol) with total lipid of 20 μmol were dissolved in chloroform. Then the chloroform was vacuumed to a lipid film for 3 h on a rotary evaporator. For traditional ammonium gradient loading, 250 mM ammonium sulfate solution was used to hydrate the lipid film to form liposomal suspension. The liposomes were extruded through polycarbonate (PC) membranes of 400, 200 and 100 nm pore sizes in sequence. The extruded liposomes were dialyzed in PBS to build the transmembrane ammonium gradient required by active loading. Finally, doxorubicin was added to the liposome suspension at a drug to lipid ratio of 1:10 (mol/mol) and incubated at RT for 30 min. The drug encapsulation efficiency was measured by detecting the fluorescence intensity of 1% Triton X-100 lysed Dox-LPs purified by a Sephadex G-25 column and compared to the unpurified counterparts.

As for SEAL method, the vacuumed lipid film was hydrated and extruded through 400 nm and 200 nm PC membranes in PBS, followed by dialysis into 250 mM ammonium sulfate hydrate. Then sonication and extrusion processes were adopted using the same conditions in preparation of Dox-mEVs. A second dialysis was applied in PBS to established the transmembrane ammonium gradient, and the following drug loading and purification operations were identical as described above. With regard to the passive incubation method, the lipid film was hydrated in PBS and directly mixed with doxorubicin at a same drug-to-lipid ratio.

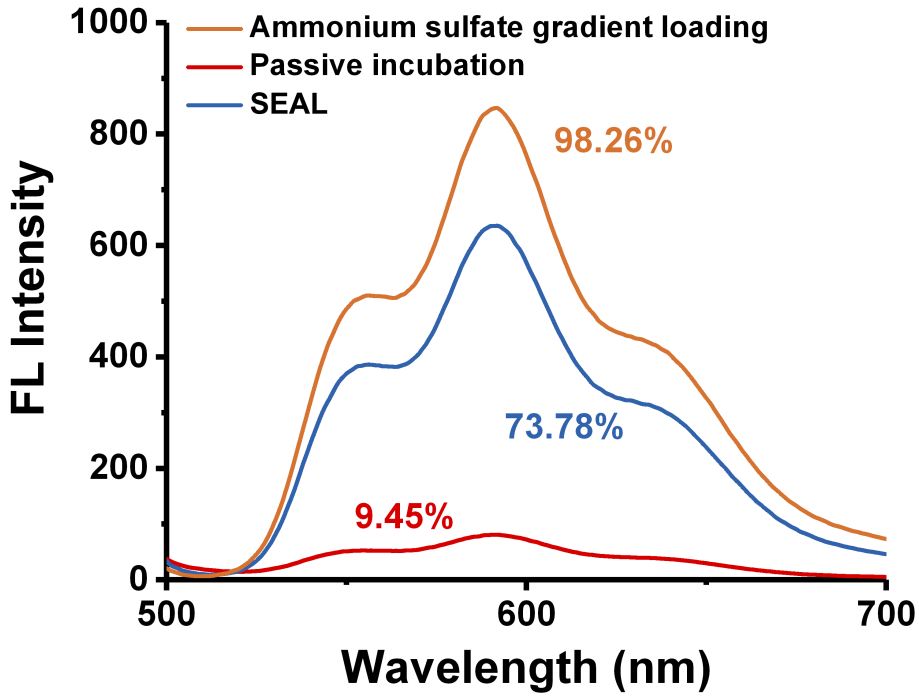

Figure S1. Fluorescence intensity of Triton X-100 lysed Dox-LPs by traditional ammonium sulfate gradient, passive incubation and SEAL. Note: the numbers were referred to the encapsulation efficiency of each method.

2. Identification of the protein markers of mEVs by western blot.

The protein concentration of the supernatant after ultracentrifugation during the mEV isolation processes, as well as the mEVs before and after SEAL were measured by BCA assay. For each sample, 80 μg protein was denatured at 100°C for 10 min before electrophoresing on a 12% polyacrylamide gel. Subsequently, the samples were transferred onto a polyvinylidene fluoride membrane using a PowerPac Basic System (Bio-Rad). The membrane was pre-blocked with 5% non-fat dry milk in TBST for 8 h at 4°C, and then was incubated with the primary antibodies at 4°C overnight. After washed seven times with TBST and incubated with horseradish peroxidase-conjugated secondary antibody, the blot was imaged by a Bioanalytical Imager c400 (Azure

Biosystems). The antibodies used for immunoblotting were purchased from Abcam: rabbit monoclonal anti-human CD9 antibody (clone EPR23105-125, dilution 1:1000), rabbit monoclonal anti-human CD63 antibody (clone EPR5702, dilution 1:1000), rabbit monoclonal anti-human CD81 antibody (clone EPR4244, dilution 1:1000), rabbit monoclonal anti-human TSG101 antibody (clone EPR7130 (B), dilution 1:1000) and rabbit monoclonal anti-human HSP70 (clone EPR16892, dilution 1:1000).

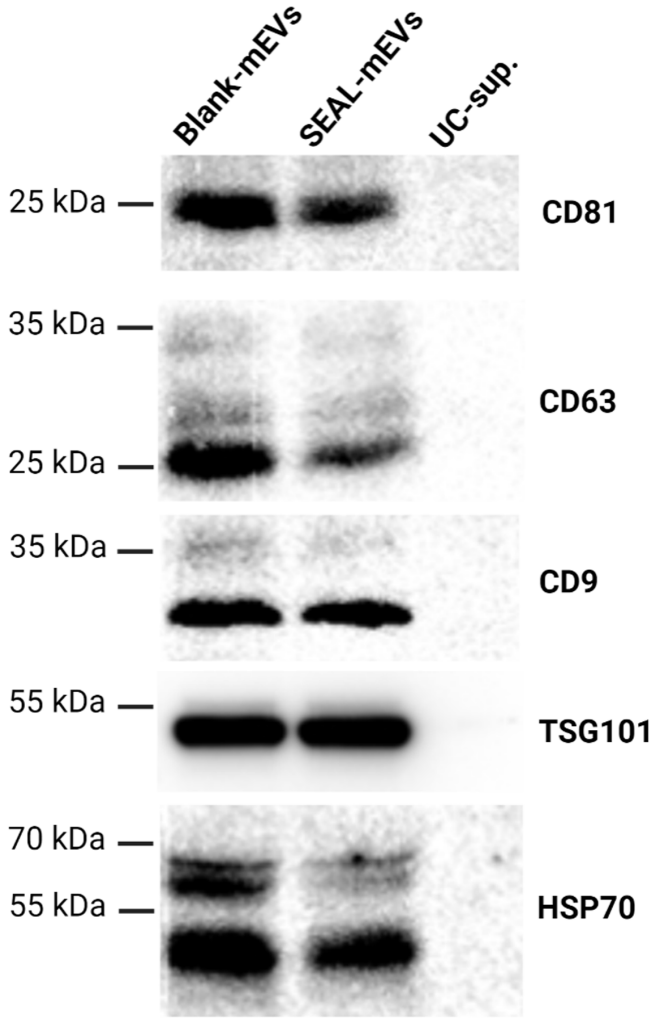

Figure S2. Western blotting analysis of UC-isolated mEVs (Blank-mEVs), mEVs after SEAL process (SEAL-mEVs) and the milk supernatant after ultracentrifugation during the isolation of mEVs (UC-sup.).

3. The impact of extrusion cycles on drug loading capacity of mEVs without sonication.

To study the impact of sole extrusion on the drug loading ability, mEVs were extruded with 100 nm PC membrane for various cycles without sonication, followed by drug loading process in accordance with the SEAL method. Then the fluorescence intensity of Dox-mEVs under various extrusion cycles were measured. It was demonstrated that two cycles of extrusion were enough to promote the buffer exchange across the membrane and increase the encapsulation efficiency.

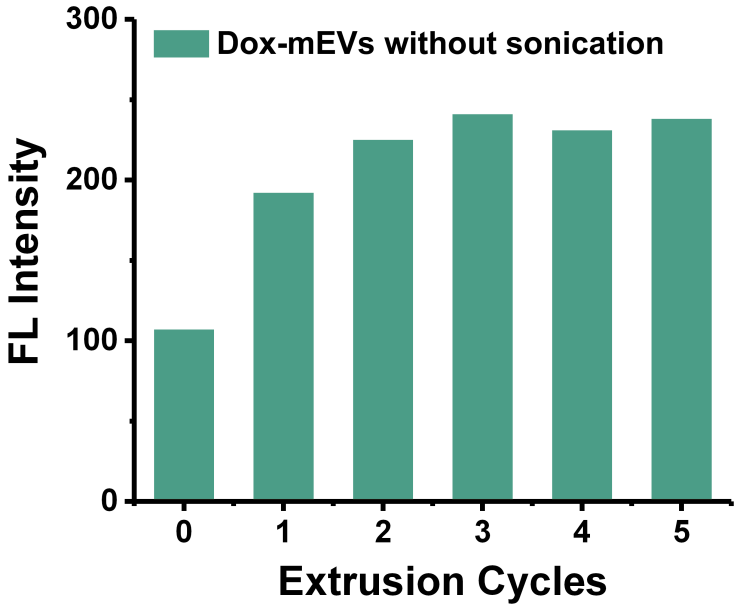

Figure S3. Fluorescence intensity of Dox-mEVs using various extrusion cycles without sonication treatment.

4. The calibration curve between doxorubicin concentration and fluorescence intensity.

To quantify the drug loading capacity of Dox-mEVs, doxorubicin solutions with concentration of 0.25 μM, 0.5 μM, 1.0 μM, 2.0 μM and 5.0 μM were used as standards to build the calibration curve.

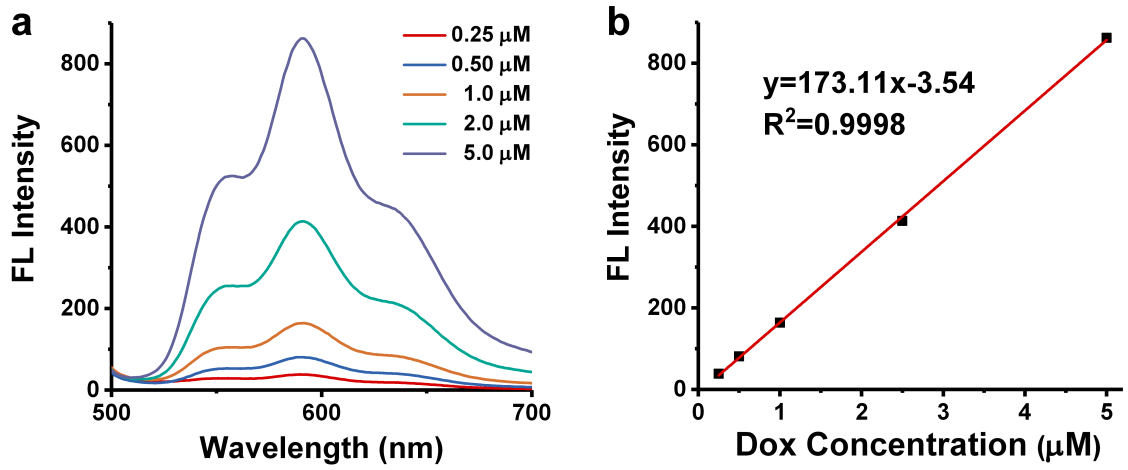

Figure S4. (a) Florescence intensity of doxorubicin solutions with various concentration. (b) The calibration curve between doxorubicin concentration and fluorescence intensity.

5. The impact of mEVs concentration on drug loading capacity of Dox-mEVs.

To study the impact of the mEVs concentration on the drug loading capacity, 200 μM doxorubicin solution was incubated with mEVs with various protein concentration. The fluorescence intensity was measured to construct the relationship between mEVs concentration and the drug loading concentration and encapsulation efficiency.

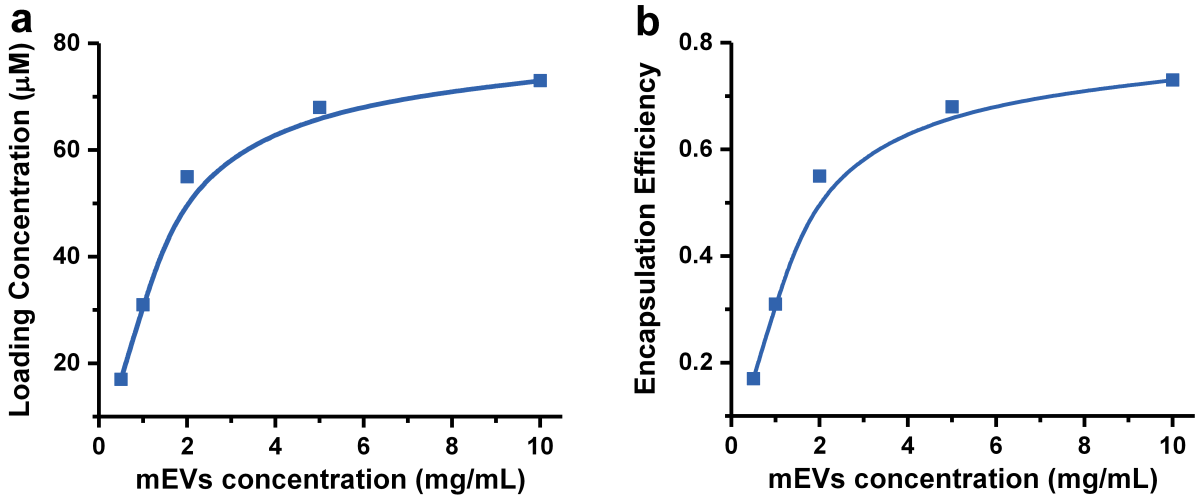

Figure S5. Measurement of the loading concentration (a) and encapsulation efficiency (b) of SEAL-prepared Dox-mEVs with various concentration.

6. Comparison of drug encapsulation efficiency between SEAL and electroporation.

The mEVs with protein concentration of 5 mg/mL were loaded with 0.2 mM doxorubicin using passive incubation (24 h, 4 °C), electroporation and SEAL. The processes of passive incubation and SEAL are described in main text. As for electroporation, doxorubicin was loaded into mEVs at 350 V and 150 μF in a 4 mm cuvette by Gene Pulser Electroporator (Bio-Rad). Recovery of the membrane enclosure of Dox-mEVs was ensured by 30 min incubation at room temperature before removing the unloaded doxorubicin.

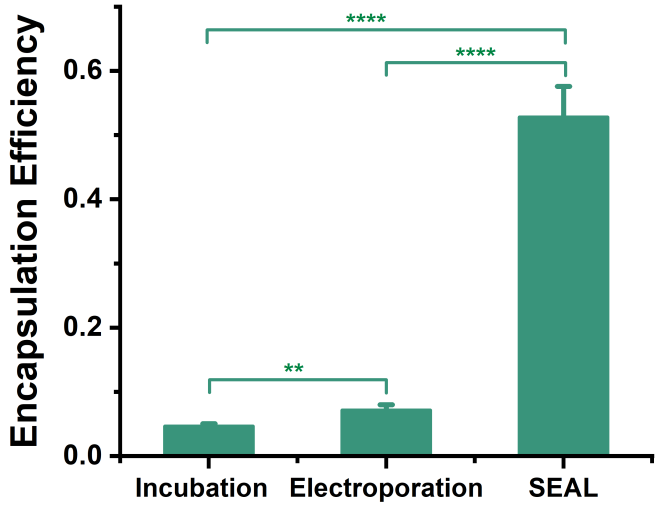

Figure S6. The encapsulation efficiency of Dox-mEVs prepared by passive incubation (24 h, 4 °C), electroporation and SEAL. P-values were calculated by t-test. **p < 0.01, ****p < 0.0001 (n = 3, mean ± SD).

7. DLS measurement of SEAL-prepared Dox-mEVs

The particle size, polydispersity index and zeta potential of the blank mEVs and SEAL-prepared Dox-mEVs were measured by dynamic light scattering (DLS).

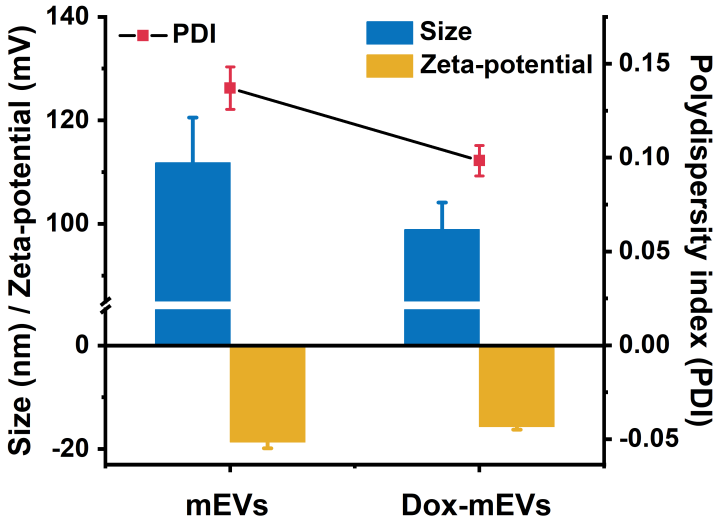

Figure S7. The particle size, PDI and zeta-potential of mEVs before and after doxorubicin encapsulation by SEAL.

8. Encapsulation of MXT and AO by SEAL.

Mitoxantrone (MXT, 0.5 mM) and acridine orange (AO, 0.5 mM) was also loaded to mEVs by SEAL method. MXT and AO loaded mEVs were lysed by 1% Triton X-100 to release the accumulated drugs or dyes. The significant fluorescence recovery after surfactant treatment confirmed the active accumulation of molecules in the lumen of mEVs.

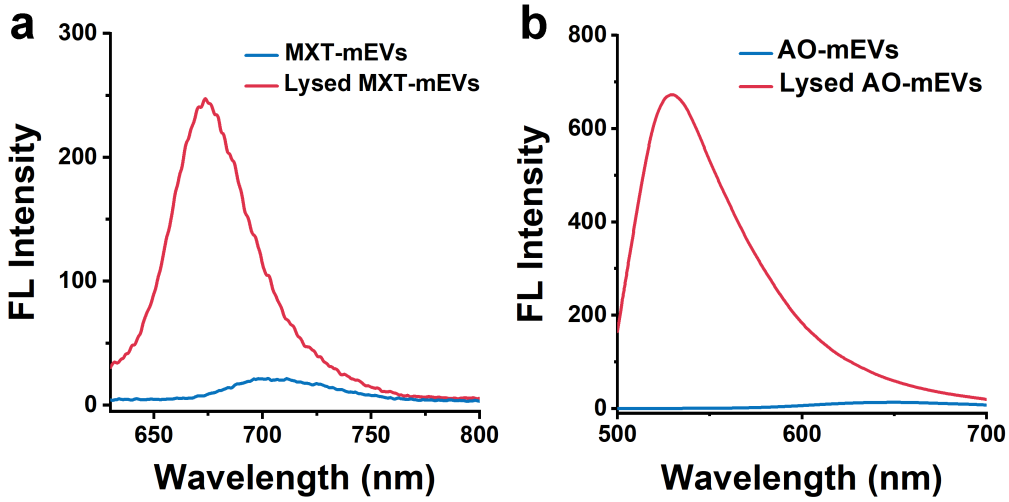

Figure S8. Fluorescence analysis of MXT-mEVs (a) and AO-mEVs (b) prepared by SEAL.

9. Size distribution measurement of Dox-mEVs by nFCM

The particle size distribution of SEAL-prepared Dox-mEVs was measured by nFCM. In brief, a mixture of monodisperse silica nanoparticles (SiNPs) with diameter of 47, 59, 74 and 94 nm was used as the standard. The calibration curve between the SS burst area and the particle size was constructed, which could be used to calculate the mEVs size distribution. Therefore, the size distribution histograms of the two subpopulations of SEAL prepared Dox-mEVs could be deciphered. It should be noted that the discrepancy of refractive index among HL-mEVs, UPL-mNPs and the SiNPs standard might compromise the accuracy of the size measurement results.

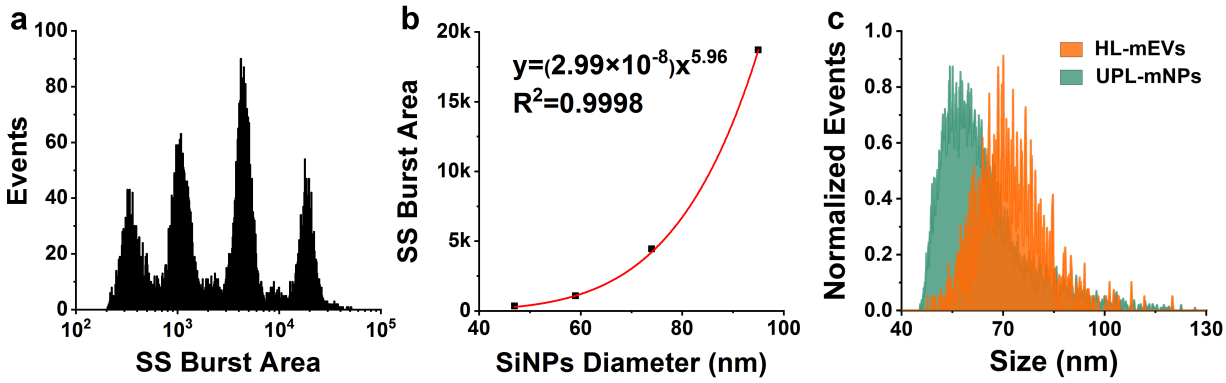

Figure. S9. Particle size distribution measurement of Dox-mEVs by nFCM. (a) SS burst area distribution histogram of silica nanoparticles (SiNPs) mixtures with diameters ranging between 47 and 95 nm. (b) The relationship between SiNPs size and SS burst area. (c) Particle size distribution of the two subpopulations of SEAL-prepared Dox-mEVs.

10. Determination of the major fractions containing mEVs

The protein concentration of each fraction of mEV formulations purified by SEC were measured by BCA assay (Figure S10a). It was determined that there were two peaks representing the EV fractions (7 to 11) and free protein fractions (17 to 25), respectively. The particle concentration of each fraction was analyzed by nFCM, and it also proved that the majority of EVs was found in fractions from 7 to 11 (Figure S10b).

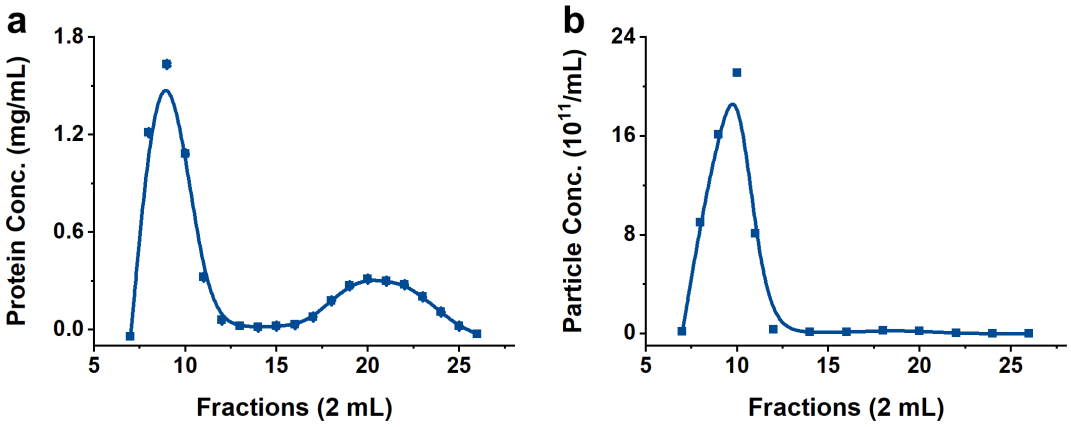

Figure S10. Determination of the major fractions containing mEVs. (a) Protein content measurement of each fraction of mEVs after SEC purification by BCA assay. (b) Particle concentration measurement of each fraction of mEVs after SEC purification by nFCM.

11. Surfactant-assisted vesicle disruption assay

For the disruption of DiD labeled Dox-mEVs, Triton X-100 was added to the samples at a final concentration of 1% and incubated for 1 h at 4 °C. The upgraded nFCM was applied for the multi-parameter correlation analysis of the lysed samples. The significant reduction in event rate verified the correlation between drug loading and lipid inclusion.

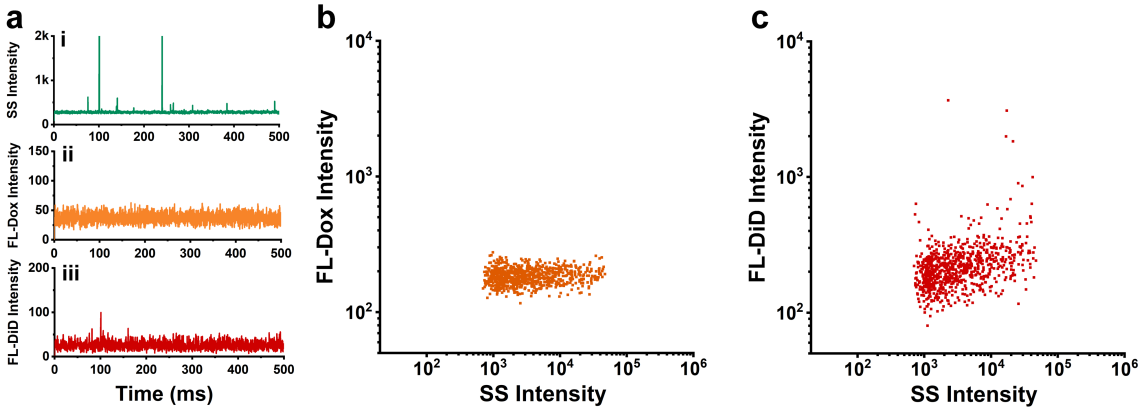

Figure S11. Multi-parameter analysis of Triton X-100 lysed mEV samples. (a) Representative SS, FL-Dox and FL-DiD burst traces of the DiD labeled Dox-mEVs lysed by Triton X-100. (b) Bivariate dot-plots of FL-Dox versus SS. (c) Bivariate dot-plots of FL-DiD versus SS.

12. Recovery rate estimation of Dox-mEVs purified via various methods

The relative abundance of Dox-mEVs prepared by SEAL before and after each purification process was estimated via single-particle enumeration by nFCM. If total particle concentration of SEAL-prepared Dox-mEVs was regarded as 100% before purification, the recovery rate was estimated to be lower than 5% for the final formulation purified by SEC and two independent magnetic separation methods, (Figure S12a). When only the actively-loaded Dox-mEVs were taken into account, this value would be increased to around 15%, since the removal of unloaded particles was more significant than the loss of the actively-loaded subpopulation (Figure S12b). It was clearly demonstrated that the SEC and IMIT processes mainly eliminated the unloaded particles without severe compromise of the actively loaded content. The significant depletion of drug-encapsulated subpopulation was occurred during the LPMIT process, where 75.4% of the actively-loaded Dox-mEVs was lost.

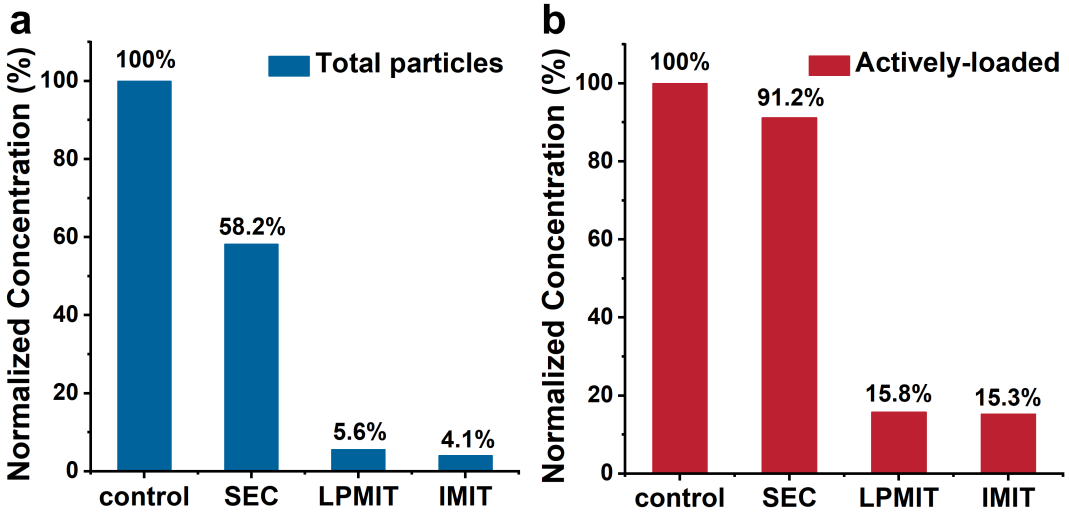

Figure S12. Estimation of the recovery rate of Dox-mEVs purified via various methods. (a) Assessment by total particle concentration; (b) Assessment by the concentration of actively-loaded subpopulation.

13. Cell cytotoxicity analysis by CCK-8

Dox-mEVs before and after transferrin conjugation with 1.0 μM drug content, as well as the mEVs control and free doxorubicin were incubated with HepG2 cells respectively to demonstrate that transferrin conjugation was capable to increase the cytotoxicity of Dox-mEVs.

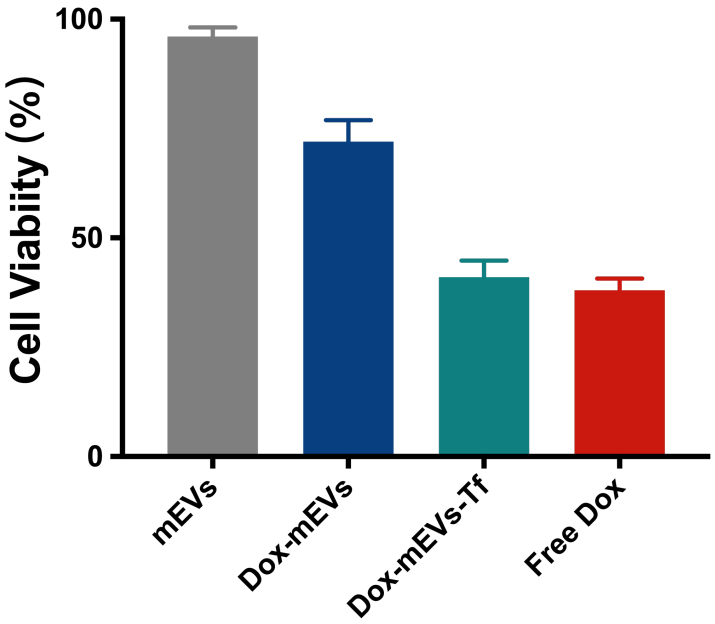

Figure S13. Cytotoxicity analysis of mEVs, Dox-mEVs, Dox-mEVs-Tf and free Doxorubicin.